Published in final edited form as:
Inorg Chem. 2007 October 29; 46(22): 9285–9293. doi:10.1021/ic7012667.

Investigating the Vanadium Environments in Hydroxylamido V(V) Dipicolinate Complexes Using ^{51}V NMR Spectroscopy and Density Functional Theory

Kristopher J. Ooms[1], **Stephanie E. Bolte**[1], **Jason J. Smee**[2,3], **Bharat Baruah**[2], **Debbie C. Crans**[2,*], and **Tatyana Polenova**[1,*]

[1]Department of Chemistry and Biochemistry, 112 Lammot DuPont Laboratories, University of Delaware, Newark, Delaware 19716

[2]Department of Chemistry, Colorado State University, Fort Collins, CO 80523

[3]Department of Chemistry, The University of Texas at Tyler, 3900 University Blvd., Tyler, Texas 75799

Abstract

Using ^{51}V magic angle spinning solid-state NMR, SSNMR, spectroscopy and quantum chemical DFT calculations we have characterized the chemical shift and quadrupolar coupling parameters of a series of 8 hydroxylamido vanadium(V) dipicolinate complexes of the general formula VO(dipic)(ONR_1R_2)(H_2O) where R_1 and R_2 can be H, CH_3, or CH_2CH_3. This class of vanadium compounds was chosen for investigation because of their seven coordinate vanadium atom, a geometry for which there is limited ^{51}V SSNMR data. Furthermore, a systematic series of compounds with different electronic properties are available and allows for the effects of ligand substitution on the NMR parameters to be studied. The quadrupolar coupling constants, C_Q, are small, 3.0 to 3.9 MHz, but exhibit variations as a function of the ligand substitution. The chemical shift tensors in the solid state are sensitive to changes in both the hydroxylamide substituent and the dipic ligand, a sensitivity which is not observed for isotropic chemical shifts in solution. The chemical shift tensors span approximately 1000 ppm, and are nearly axially symmetric. Based on DFT calculations of the chemical shift tensors, one of the largest contributors to the magnetic shielding anisotropy is an occupied molecular orbital with significant vanadium d_z2 character along the V=O bond.

Keywords

Solid-State NMR; Magic Angle Spinning; MAS; ^{51}V; hydroxylamido complexes; dipicolinic acid; quadrupolar; chemical shift; magnetic shielding; EFG; CSA

[*1]Tatyana Polenova, Department of Chemistry and Biochemistry, University of Delaware, Newark, DE 19716, tpolenov@mail.chem.udel.edu, Tel. (302) 831-1968, FAX (302) 831-6335. [2]Debbie C. Crans, Department of Chemistry, Colorado State University, Fort Collins, CO 80523, crans@lamar.colostate.edu, Tel: (970) 491-7635, FAX: (970) 491-1801.

Introduction

Studies have shown that vanadium, while a trace element in biochemical systems, can play an important role in metalloenzymes and impact insulin regulation.[1, 2, 3] One class of compounds that are insulin enhancing agents are vanadium dipicolinate complexes.[4, 5, 6, 7, 8] In these compounds the vanadium likely plays an important role in determining the biological activities[9, 10, 11] and ligand functionalization can be used to tune the properties of these complexes.[12] The parent five-coordinate dipicolinate vanadium complexes can form adducts with small ligands such as peroxides and hydroxylamines.[1, 13, 14] Studies of systematic series of ternary vanadium complexes that are known to contain two different coordinating ligand systems can assist in gauging the effect of ligand substitution on the chemistry at the vanadium center. Solid-state ^{51}V NMR has the potential to yield a three-dimensional description of the local vanadium environment and of the possible changes that take place in the molecular orbitals and electrostatic structure at the vanadium when the coordinating ligands are changed.[3, 15, 16, 17, 18, 19, 20]

Many inorganic vanadium–containing coordination complexes have been studied using ^{51}V SSNMR.[21, 22, 23] The investigations of vanadium organometallic and coordination compounds have illustrated that valuable information about the molecular and electronic structure can be obtained by measuring the anisotropy of the ^{51}V chemical shift tensor and the electric field gradient (EFG) tensor; ^{51}V is a spin I = 7/2 quadrupolar nucleus.[24, 25, 26] The ^{51}V chemical shifts span a range of approximately 3500 ppm making it a sensitive probe of structure.[19] Typical quadrupolar coupling constants, C_Q, are small compared to many other half-integer quadrupolar nuclei because of the small nuclear quadrupole moment of ^{51}V, −4.8 fm^2;[27] C_Q values for highly coordinated vanadium sites are typically less than 15 MHz.[19, 21, 28] ^{51}V solid-state NMR spectroscopic studies of the active site of vanadium chloroperoxidase enzymes have provided insights such as details about the protonation mechanism of the peroxide.[3, 20] In general, many of these studies have illustrated that the anisotropy of the ^{51}V chemical shift tensor is more informative than the isotropic chemical shifts alone.[28]

Modern quantum chemical calculations have proven invaluable for understanding the origins of the NMR parameters in transition metal complexes.[29, 30, 31] Calculations of ^{51}V NMR parameters have been performed for a range of vanadium compounds and have employed both single-molecule and extended-structure models.[26, 27, 32, 33, 34] These studies have suggested that in non-ionic coordination complexes, both the magnetic shielding and the EFG tensors are predominantly determined by the local structure about the vanadium, and that the extended crystal lattice plays only a minor role. Good agreement between experimental and calculated NMR parameters has been obtained for vanadium.[26] To better understand the relationships between the NMR parameters and the reactivity at the vanadium center, more experimental and computational NMR investigations of systems with variations in the electronic properties of ligands and vanadium are required.

In this work, we have investigated a series of eight seven-coordinate hydroxylamido vanadium(V) dipicolinate (dipic) complexes, Figure 1, using ^{51}V solid-state and solution NMR spectroscopy, and quantum chemical DFT calculations. The compounds differ in the

functionality at either the hydroxylamido ligand (hydrogen replaced with methyl, Me, or ethyl, Et, groups) or the dipic ligand, which was substituted in the para position with respect to the nitrogen of the ring. Single-crystal x-ray diffraction studies reveal that there is one unique molecule in the unit cell, and that in addition to the dipic and hydroxylamido ligands, a water molecule is trans to the V=O bond with a bond length of approximately 2.45 Å.[37] This is a very long bond, and likely to be weak. Interestingly, the comparison of experimental solid-state and solution NMR spectroscopic chemical shifts demonstrates that ligand-associated changes lead to a greater variation in the anisotropic tensors than in the isotropic values. The combined experimental and computational results reveal that in this series, the quadrupolar coupling constants and chemical shift anisotropies display a relatively small variation when the ligand is substituted.

Experimental

Sample preparation

Sodium metavanadate (96%), potassium permanganate and hydroxylamine hydrochloride ($NH_2OH{\cdot}HCl$) were purchased from Fisher Scientific. Ammonium metavanadate (99%), potassium metavanadate (98%), dipicolinic acid (also referred to as 2,6-pyridinedicarboxylic acid, H_2dipic), *N*-methylhydroxylamine hydrochloride (MeNHOH·HCl), *N*, *N*-dimethylhydroxylamine hydrochloride ($Me_2NOH{\cdot}HCl$) and aqueous *N*, *N*-diethylhydroxylamine (Et_2NOH, 85% w/w) were purchased from Aldrich. Chelidamic acid (4-hydroxy-2,6-dipicolinic acid) monohydrate was purchased from TCI America. The $NH_4[VO_2(dipic)]$ complex,[35] $Na[VO_2(dipic\text{-}OH)]{\cdot}2H_2O$,[36] and $[VO(dipic)(ONH_2)(H_2O)]$[37] were prepared as previously reported. The $(NH_4)_2$dipic-NH_2 was prepared modifying a previously reported synthesis.[38] Sodium 4-aminodipicolinatooxovanadate(V) dihydrate, $Na[VO_2(dipic\text{-}NH_2)]{\cdot}2H_2O$ was prepared similarly as reported previously for the NH_4^+ salt.[4] IR spectroscopy on the compounds was carried out (either as KBr pellets, or as Nujol mulls on NaCl plates) on an Avatar 320 FTIR. Elemental analysis (C, H, N) was carried out by Desert Analytics in Tucson, Arizona.

Aquadipicolinatohydroxylamidooxovanadium(V) $[VO(dipic)(ONH_2)(H_2O)]$ (1)— The compound was prepared as described previously.[37] ^{1}H NMR (D_2O, ppm): 8.63 (t), 8.39 (dd, 2H). ^{51}V NMR (D_2O, ppm): –681.

Aquadipicolinatomethylhydroxylamidooxovanadium(V), $[VO(dipic)(ONHMe)(H_2O)]$ (2)—The compound was prepared as described previously by first preparing the $NH_4[VO_2(dipic)]$ complex[35] from $NaVO_3$ and H_2dipic.[13] ^{1}H NMR (D_2O, ppm): 8.64 (t, 1H), 8.39 (dd, 2H), 3.90 (s, 3H), 3.43 (s, 3H). ^{51}V NMR (D_2O, ppm): –634, –647.

Aquadipicolinatodimethylhydroxylamidooxovanadium(V) 0.5 hydrate $[VO(dipic)(ONMe_2)(H_2O)]{\cdot}0.5H_2O$ (3)—The compound was prepared analogous to **2** using $Me_2NOH{\cdot}HCl$ in place of MeHNOH·HCl as described previously by first preparing the $NH_4[VO_2(dipic)]$ complex[35] from $NaVO_3$ and H_2dipic.[13] ^{1}H NMR (D_2O, ppm): 8.62 (t, 1H), 8.38 (dd, 2H), 3.95 (s, 3H), 3.42 (s, 3H). ^{51}V NMR (D_2O, ppm): –614.

Aquadipicolinatodiethylhydroxylamidooxovanadium(V) [VO(dipic)($ONEt_2$)(H_2O)] (4)—The compound was prepared analogous to **2** using Et_2NOH in place of MeHNOH·HCl as described previously by first preparing the $NH_4[VO_2(dipic)]$ complex[35] from $NaVO_3$ and H_2dipic[13] ^1H NMR (D_2O, ppm): 8.62 (t, 1H), 8.38 (dd, 2H), 3.87 (m, 2H), 3.44 (m, 2H), 1.59 (t, 3H), 1.41 (t, 3H). ^{51}V NMR (D_2O, ppm): –598.

Ammonium 4-aminodipicolinate, $(NH_4)_2$(dipic-NH_2)—The ligand was prepared modifying the literature procedure[38] as described in by Smee et. al..[13] ^1H NMR (D_2O, pH 7.0, ppm): 7.13 (s, py-*H*, 2H).

Sodium 4-aminodipicolinatodioxovanadate dihydrate, Na[VO_2(dipic-NH_2)]·$2H_2O$—Na[VO_2(dipic-NH_2)]·$2H_2O$ was prepared similarly as previously reported for the NH_4^+ salt.[4, 13] ^1H NMR (D_2O, ppm): 7.1 (s, py-*H*, 2H). ^{51}V NMR (D_2O, ppm): –525.

Aqua-4-aminodipicolinatohydroxylamidooxovanadium(V) [VO(dipic-NH_2)(ONH_2)(H_2O)] (5)—The compound was prepared as described previously from Na[VO_2(dipic-NH_2)]·$2H_2O$.[13] ^1H NMR (D_2O, ppm): 7.20 (s, 2H). ^{51}V NMR (D_2O, ppm): –688.

Aqua-4-aminodipicolinatodimethylhydroxylamidooxovanadium(V) monohydrate [VO(dipic-NH_2)($ONMe_2$)(H_2O)]·H_2O (6)—The compound was prepared using an analogous procedure to **5** using Me_2NOH·HCl instead of H_2NOH·HCl as described previously from Na[VO_2(dipic-NH_2)]·$2H_2O$.[13] ^1H NMR (D_2O, ppm): 7.20 (dd, 2H), 3.81 (s, 3H), 3.28 (s, 3H). ^{51}V NMR (D_2O, ppm): –619.

Aqua-4-aminodipicolinatodiethylhydroxylamidooxovanadium(V) [VO(dipic-NH_2)($ONEt_2$)(H_2O)] (7)—The compound was prepared using an analogous procedure to **5** using Et_2NOH instead of H_2NOH·HCl as described previously from Na[VO_2(dipic-NH_2)]·$2H_2O$. [13] ^1H NMR (D_2O, ppm): 7.18 (dd, 2H), 3.71 (m, 2H), 3.35 (m, 2H), 1.43 (t, 3H), 1.26 (t, 3H). ^{51}V NMR (D_2O, ppm): –604.

Aqua-4-hydroxydipicolinatomethylhydroxylamidooxovanadium(V) [VO(dipic-OH)(ONHMe)(H_2O)]·H_2O (8)—The [VO(dipic-OH)($ONMe_2$)(H_2O)] was prepared most consistently by using Na[VO_2(dipic-OH)]·$2H_2O$ prepared as described previously.[36] Na[VO_2(dipic-OH)]·$2H_2O$ (0.32 g, 0.99 mmol) was dissolved in H_2O (50 ml). MeHNOH·HCl (0.083 g, 1.0 mmol) was added to it and the clear solution was allowed to stir for 1 hour. A light yellow solution of pH ~3 was kept at 4°C for 72 hrs. The precipitate, which had formed, was filtered off and vacuum dried. Yield: 0.15 g (50%). IR (NaCl, ν(COO), ν(V=O)), cm^{-1}): 1653 (br,s), 1461 (s), 1377 (vs), 1064 (vs), 994 (m). ^1H NMR (D_2O, pH 2.68): 7.61 (dd, 2H), 3.88 (s, 3H), 3.4 (s, 3H). ^{51}V NMR (D_2O, pH 2.68): –637, –650. Calcd for $C_8H_9N_2O_8V$: C 25.60, H 3.76, N 8.05. Found: C 27.63, H 3.49, N 7.89.

Solution Preparation and Solution State ^{51}V NMR Spectroscopy

The ^1H and ^{51}V spectra were recorded on a Varian INOVA-300 spectrometer (7.0 T) at 300 MHz for ^1H and 78.9 MHz for ^{51}V. Routine parameters were used for the ^1H NMR spectra

and DSS (3-(trimethylsilyl)-propanesulfonic acid, sodium salt) was used as the external reference for the ^{1}H chemical shifts. The ^{51}V NMR spectra were generally acquired with a spectral window of 83.6 kHz, a pulse angle of 60° and an acquisition time of 0.096 s with no relaxation delay. The ^{51}V chemical shifts were obtained using an external reference of $VOCl_3$, δ_{iso} = 0.00 ppm.

Solid-State NMR spectroscopy

Solid-state ^{51}V NMR spectra were acquired on a Tecmag Discovery spectrometer, interfaced with a wide bore 9.4 T Magnex magnet, and operating at a frequency of 105.23 MHz for ^{51}V. Vanadium chemical shifts were referenced to neat $VOCl_3$, δ_{iso} = 0.0 ppm, as an external reference.[39] This sample was also used to determine the 90° pulse widths of 4.0 μs ($\delta B_1/2\pi \approx 62$ kHz). The magic angle, MA, was set by maximizing the number of rotational echoes observed in the ^{23}Na NMR free induction decay of solid $NaNO_3$. The angle was set for each sample; accurate setting of the MA is critical when acquiring spectra from the satellite transitions of quadrupolar nuclei over a broad frequency range.[21] A 4 mm Doty XC4 MAS probe was used for acquiring all the spectra. For each sample, spectra at several MAS frequencies ranging from 11 to 17 kHz were collected. The MAS frequency was controlled by an automated Tecmag MAS Control Unit to within 5 Hz. All spectra were acquired using a one-pulse experiment with a pulse of 1μs, a spectral width of 2 MHz, and a recycle time of 1 s. Proton decoupling did not significantly improve the spectra and was therefore not used. The NMR spectra were processed with Gaussian line broadening functions of 100 Hz, and baseline corrections. Spectra of the entire manifold of central and satellite transitions were simulated with SIMPSON,[40] using 1 μs excitation pulses at a 62 kHz B_1 field; these settings match the experimental conditions.

Computations

Gaussian03[41] was used to calculate the vanadium magnetic shielding and EFG tensors. The B3LYP[42, 43] functional and the 6-311+G(p,d) basis set were employed for all atoms, as available in the Gaussian package; molecular orbitals and electrostatic potential surfaces were displayed using GaussView3.09.[44] Natural bond order, NBO,[45] analysis and natural chemical shielding, NCS,[46] analysis were also performed using Gaussian03. The calculated principal components of the magnetic shielding tensor, σ_{ii} (i = 1, 2, or 3), were converted to the principal components of the chemical shift tensor, δ_{ii}, using the relation $\delta_{ii} = \sigma_{iso}$ (ref) − σ_{ii}, where σ_{iso} (*ref*) = −2286 ppm and is the calculated isotropic magnetic shielding of $VOCl_3$. The structures used in the calculations were obtained from single-crystal x-ray diffraction data[37, 13] or the geometry optimized structure of $VOCl_3$; optimization was performed using B3LYP/6-311+G(d,p). Carbon-hydrogen bond lengths were set to 1.08 and 1.09 Å for carbons bonded to three and four other atoms, respectively. Nitrogen-hydrogen and oxygen-hydrogen bond lengths were set to 1.06 and 0.96 Å, respectively. [47]

Results

Hydroxylamido Vanadium(V) Dipicolinate Complexes

A number of vanadium(V) hydroxylamido complexes have been prepared, all containing seven-coordinate vanadium atoms. Although the vanadium complex is susceptible to

hydrolysis and reduction, preparation of the parent vanadium dipicolinate complex prior to addition of hydroxyl amine significantly reduces the amount of redox chemistry and side-product formation. All the complexes described in this manuscript have been prepared by this method. Details of the preparation and solution properties of this class of compounds have been described elsewhere.[13] However, in this manuscript we provide sufficient information to allow a comparison of the aqueous solution and solid state NMR chemical shifts.[13]

Solid-State ^{51}V NMR spectroscopy

For each of the samples, ^{51}V NMR spectra were acquired at 9.4 T using several MAS rates (ν_{rot}). Figure 2 shows the spectra acquired of V(V)O(dipic-OH)(ONHMe)(H_2O), **8**, when the sample was spun at 11 kHz, 15 kHz and 17 kHz. The isotropic chemical shifts are indicated with asterisks in Figure 2. The use of different MAS rates allows for accurate determination of the anisotropic observables from numerical simulations. Figure 3 shows a representative spectrum of VO(dipic)(ONH_2)(H_2O), **1**, acquired at the MAS frequency of 11 kHz, along with an expansion of the central region of the spectrum. From the expansion it can be seen that each spinning side band has a nearly isotropic lineshape, and the center-band, δ_{iso}, is near −71 kHz (−677 ppm). The isotropic lineshapes of the individual spinning side bands indicate that the ^{51}V C_Q is small, probably less than 4 MHz, which results in no noticeable second-order quadrupolar lineshape at 9.4 T. The small C_Q values also lead to small second-order quadrupolar shifts which cause the center-bands from the various transitions to overlap; the small shoulder on the high frequency sides of the peaks, Figure 3 inset, is from the small difference in the shifts of the different transitions. The ^{51}V δ_{iso} values can therefore be easily obtained from the centerband because any second order quadrupolar shifts are small. However, the small C_Q values mean that the quadrupolar coupling constants cannot be obtained by fitting the lineshapes of the individual central-transition spinning side bands as is commonly done for quadrupolar nuclei, but rather the entire spinning side band manifold, spanning the central and satellite transitions, needs to be examined as discussed below.

The overall shape of the spinning side band envelope is dominated by the contribution of the first-order quadrupolar interaction to the ^{51}V NMR satellite transitions. Due to the small C_Q, the ^{51}V NMR signal in this series under investigation originates from both the satellite transitions (m_I = ±7/2↔±5/2, ±5/2↔±3/2, ±3/2↔±1/2), light grey spectrum in Figure 3, and the central transition (m_I =+1/2↔−1/2), the dark grey spectrum in Figure 3. The central transition is not affected by the quadrupolar interaction to first order and consequently, the influence of the chemical shift anisotropy is readily apparent in this region.[48] The spinning side bands from the central transition span approximately 100 kHz and display a pattern typical of an axially symmetric chemical shift tensor.

By fitting calculated spectra to the experimental spectra, Figure 4 and 5, the ^{51}V NMR parameters can be obtained: the C_Q and η_Q parameters can be determined primarily from the satellite transitions, which exhibit only small affects of the chemical shift parameters, while the chemical shift parameters can be determined from the central transition, which exhibits only minor contributions from the second-order quadrupolar interaction. The ^{51}V NMR

observables for the eight samples studied here are presented in Table 1; definitions of the NMR parameters used can be found in the footnote of Table 1. The chemical shift tensors are nearly axially symmetric ($\delta_{11} \approx \delta_{22}$) for all complexes with spans ($\delta_{11} - \delta_{33}$) of approximately 930 to 1120 ppm. The principal components of the chemical shift tensor are indicated in the expansion of the spectrum acquired for VO(dipic)(ONH_2)(H_2O) at 17 kHz spinning frequency, see Figure 3. The C_Q values are all between 3.0 and 3.9 MHz with η_Q values between 0.4 and 0.8.

he relative orientation of the two tensors also plays a pronounced role in determining the lineshape of the spinning side band envelope, particularly the angle between δ_{33} and V_{ZZ}, β (see reference 49 for a discussion of the Euler angle convention used). In general the lineshapes were fit best using an α angle of 10 to 50° ± 30° for different samples while the β angle was 90°± 20°;[50] γ had no significant effect due to the near axial symmetry of the chemical shift tensor.

Quantum chemical calculations

Crystal structures obtained from single-crystal x-ray diffraction were available for three of the eight complexes.[13, 37] These structures were used to calculate the magnetic shielding and the EFG tensors at the vanadium nucleus. Overall, the results presented in Table 2 indicate that the calculations are in reasonable agreement with experiment. The C_Q values are all within 0.8 MHz of the experimental values; however, the asymmetry parameter of the EFG tensor is not well reproduced by the calculations. This is not a surprising result in light of prior reports demonstrating that DFT calculations at the single molecule or small cluster level may not be able to define the principal components of the EFG tensor well.[29, 30] In the compounds under investigation, since the C_Q is so small, any errors in calculating the principal components of the EFG tensor could result in large errors in the calculated asymmetry. In contrast, the axial symmetry and isotropic values of the magnetic shielding tensor are reproduced by the calculations while the calculated anisotropy of the tensor is consistently greater than that observed experimentally. By comparing the principal components of the chemical shift tensor, see Figure 6, it can be seen that most of the discrepancy between calculated and experimental chemical shift parameters lies in the most shielded component, δ_{33}. Note that δ_{11} has a deviation within experimental error, δ_{22} deviates by 100 to 150 ppm, while δ_{33} deviates by 330 to 430 ppm. Previously, quantum chemical calculations of the chemical shift anisotropy of vanadium coordination complexes have shown good agreement with experiment for complexes with O and N coordinated to the V.[26]

The orientation of the tensors in the molecular frame, which is not available from the NMR experiments, has also been obtained from the calculations. However, given the errors in the EFG asymmetry parameter the reliability of the EFG orientation obtained from the calculations is questionable. On the other hand, since the axial symmetry of the magnetic shielding is well reproduced by the calculations it is expected that the orientation of the tensor is also qualitatively correct, despite the errors in δ_{33} noted above. Only the unique component of the nearly axially symmetric tensor needs to be specified to fix the orientation of the tensor in the molecular frame. Figure 7 shows the orientation of σ_{33} in compound **1**;

calculations indicate that the orientation is the same in all three complexes for which calculations were performed. σ_{33} is perpendicular to the dipic plane and approximately coincident with the V=O bond. This orientation is similar to that previously observed for vanadium in $(NH_4)[VO(O_2)(H_2O)(dipic)]$.[26]

The sign of C_Q is another parameter not available from ^{51}V NMR spectroscopy but available from the DFT calculations. The calculations indicate that C_Q is positive for all three complexes.

Discussion

In the drive to optimize the biological activity of vanadium containing compounds the coordinating ligands can be functionalized to tune properties such as solubility, physiological uptake, and the stability of the complex under physiological conditions. Defining how the electronic properties at the vanadium center change, will assist in fine-tuning complex design. By characterizing a series of ternary complexes, changes in two different ligand systems can be monitored and the influence of each substituent on the vanadium center can be established. These hydroxylamido vanadium(V) dipicolinate complexes are of interest because the ternary complexes contain hydroxylamido and dipicolinate ligands, and the vanadium atom is seven coordinate; previous SSNMR studies have mostly focused on other coordination geometries. Furthermore, the solution ^{51}V NMR studies of these compounds demonstrated that the isotropic chemical shifts change upon modification of the hydroxylamido ligand, whereas only small changes were observed when the dipicolinate group was functionalized. However, knowledge of the isotropic chemical shifts in solution are insufficient for deriving information about the three-dimensional electronic and geometric structure of the vanadium site,[20, 26] and therefore the anisotropic EFG and chemical shift tensor parameters measured here by SSNMR and calculated using DFT are important.

The compounds studied here can be divided into two sets for comparison, compounds where the protons on the hydroxylamine are changed with alkyl groups, and compounds containing different substituents in the para position of the dipic ligand. For compounds **1** to **4** the hydroxylamido ligand is ONH_2, ONHMe, $ONMe_2$, and $ONEt_2$, respectively, see Figure 4. In general, there is a very minor change in the electric field gradient upon alkylation of the hydroxylamine: the C_Q values are 3.4, 3.0, 3.2, and 3.3 MHz; the differences are close to the experimental error. Compounds **5** to **7** also have different hydroxylamido groups but have a functionalized dipic (dipic-NH_2). For these ONH_2, $ONMe_2$, and $ONEt_2$ complexes the C_Q values are 3.9, 3.4 and 3.5 MHz, respectively, also revealing a very small variation in the EFG tensor at the vanadium site. Similarly, we observed only a small change in the EFG tensor when the substituent on the dipic ligand is modified. Samples **3, 6** and **8** have H, NH_2, and OH groups para to the nitrogen of the dipic ring, and their C_Q values were found to be 3.4, 3.9, and 3.2 MHz, respectively, see Figure 5 and Table 1. These results indicate that changing the functionality of the hydroxylamine or the dipic has a relatively small effect on the electrostatic environment at the vanadium.

We note that the EFG is the second derivative of the electric potential and the tensor is determined by the partial charge distribution around the vanadium atom, and has an $\langle r^{-3} \rangle$ dependence.[22, 26] As mentioned, the quadrupolar couplings in these compounds are relatively small considering they do not adopt octahedral or tetrahedral coordination geometries; perfect octahedral and tetrahedral geometries would produce no EFG at the vanadium.[51] By examining the electrostatic potential surface insights into the origin of the small EFGs can be gained. Figure 8 shows the ESP surface of compound 1. As can be seen the five coordinated oxygens create similar potentials about them (the blue in Figure 8 indicates regions that attract negative charge). In comparison, the potentials are much smaller in the proximity of the nitrogen atoms (green color). Given the small potentials at the nitrogens, and despite the 7-coordinate bicapped-pentagonal coordination geometry the potential surface in the immediate coordination environment about the vanadium can be best described as either a distorted trigonal prism or capped square planar arrangement. Point charge geometries such as trigonal prism, trigonal-bipyramidal and capped square planar produce small to moderate EFGs.[51] The small additional charges from the nitrogens and the extended structure will serve to increase the spherical symmetry of the charge about the vanadium, decreasing the EFG even further.

The small variations in the EFG between the different compounds suggest that the changes in functionality produce almost no change in the charge distribution of the coordinating O and N atoms from the dipic or hydroxylamine ligands; there was negligible change in the electrostatic potential surfaces near the vanadium in compounds **1, 2** and **3**. For the complexes that have different hydroxylamine ligands this observation may not be surprising given the fact that the substituent groups have similar electronegativity, H, CH_3 and CH_2CH_3. It is interesting that substitution on the dipic ligand, with the NH_2 and OH replacing the H, does not perturb the EFG at the vanadium site, again indicating very minor changes in the charge distribution close to the vanadium. These observations have important consequences because they suggest that ligand functionality in this class of compounds can be tuned for specific biological applications without causing a large change in the electrostatic environment of the vanadium.

The anisotropy of the vanadium CS tensors shows stronger variation than the EFG tensors. Of the three principal components of the CS tensor, δ_{33} exhibits the greatest variation, 238 ppm, while δ_{11} and δ_{22} show variations of 79 and 106 ppm, respectively, see Table 1. We note that the experimental error is approximately ± 30 ppm. In general, δ_{33} increases as the hydroxylamine is changed through the series ONH_2, $ONMe_2$, and $ONEt_2$. This trend was observed for the dipic, **1, 3**, and **4**, and dipic-NH_2, **5–7**, series of compounds, where δ_{33} varies by 128 and 109 ppm, respectively. Comparison of the results for the two sets of compounds indicates that δ_{33} decreases by approximately 100 ppm when the dipic is changed to dipic-NH_2, see Table 1. A larger decrease in δ_{33} of 194 ppm is observed when the dipic is replaced by dipic-OH, compounds **2** and **8**. Since δ_{33} arises from the mixing of orbitals perpendicular to the V=O bond, *vide infra*, the changes in δ_{33} arise from changes in the molecular orbitals in the dipic plane as the functionality of the dipic and oxyamide ligands are changed. This means that δ_{33} can provide insights into the molecular orbitals that are responsible for the ligand-V binding in these compounds.

In biological environments, these vanadium compounds are exposed to solvent, metabolites and other biological components. Therefore, a comparison of the solid-state and solution chemical shifts is relevant; Table 2 contains selected δ_{iso} values measured in aqueous solution.[13] Figure 9 shows a plot of solution vs. solid-state δ_{iso} and reveals that the differences are all less than 30 ppm, likely due to solvent effects. It has been suggested that for vanadium complexes with weakly bound ligands, such as the H_2O in these compounds, thermal and solvent effects are on the order of a few dozen ppm.[34] The pairs of compounds that have the same hydroxylamine ligand are illustrated using the same symbols in Figure 9. This plot clearly illustrates the small changes in the solution δ_{iso} values when the dipic ligand is varied whereas the solid-state δ_{iso} values are more sensitive to dipic substitution. Both the solution and solid-state δ_{iso} values are sensitive to changes in the hydroxylamine. Interestingly, there is a smaller difference in δ_{iso} between the methyl and ethyl substituted complexes than between the H and alkyl complexes.

For all the compounds studied, the vanadium chemical shift tensors are axially symmetric within experimental error. Upon examining the structures of the compounds, we see no obvious reason for this symmetry since the vanadium is not on a C_n rotation axis, $n \geq 3$. However, the quantum chemical calculations of the magnetic shielding tensor reproduce the axial symmetry observed experimentally and, as mentioned, the orientation of the tensor is such that the unique component of the tensor, δ_{33}, is approximately perpendicular to the plane of the dipic ligand, Figure 7.

To properly understand the chemical shift tensor one must examine the contributions of the individual molecular orbitals, MOs, to the magnetic shielding. According to the Ramsey's theory, the magnetic shielding can be divided into diamagnetic and paramagnetic terms.[52] The diamagnetic contribution to shielding, which is normally positive, depends on the ground electronic state of the molecule and is fairly constant for a given nucleus. The paramagnetic contribution to shielding, σ^p, which is normally negative, is related to the magnetic-dipole allowed mixing between symmetry-appropriate occupied and unoccupied MOs.[52, 53] Efficient mixing requires that the symmetries of the occupied MOs after a rotation about the axis of the applied magnetic field be the same as those of the unoccupied MOs. For example, when the applied magnetic field is directed along the *X*-axis, paramagnetic shielding is created when the occupied MOs with d_{xz} character mix with unoccupied MOs of d_{xy} character.[53] The energy separating the occupied and unoccupied MOs is also important, with the σ^p being inversely related to the energy difference; therefore only the MOs near the HOMO-LUMO gap are typically important for determining σ^p. Also, σ^p contains a $\hat{L}/\langle r^3 \rangle$ term, implying that only orbitals near the vanadium need to be considered. Therefore, by examining the symmetry of the occupied and unoccupied MOs near the HOMO-LUMO gap that contain significant metal *d*-character, the magnetic shielding and the orientation of the tensor can sometimes be explained.[30, 54, 55]

The natural bond order and natural chemical shielding analysis as available in Gaussian03 were used to obtain the contributions of various MOs to the isotropic vanadium magnetic shielding of $[VO(dipic)(ONH_2)(H_2O)]$ as well as the contributions from the various atomic orbitals to the MOs.[41, 45, 46] The symmetry of the MOs and percent vanadium *d*-orbital

character were then compared to the MOs generated from the DFT magnetic shielding calculations to gain an understanding of which MOs contribute to the magnetic shielding.

Figure 10 shows the four occupied [VO(dipic)(ONH_2)(H_2O)] MOs that contribute the most to the vanadium σ^{p}_{iso}. As illustrated in the figure, the MOs can be said to have symmetries closely related to the vanadium *d*-orbitals. The largest single contributor to the shielding is an occupied MO that displays significant d_z2 character, Figure 10a; the axis system is fixed such that *Z*-axis is perpendicular to the dipic plane. Mixing of the MO depicted in Figure 10a with unoccupied MOs of the appropriate symmetry accounts for 25% of the total σ^{p}_{iso}. The d_z2 orbital is unique among the *d*-orbital symmetries in that it does not produce paramagnetic shielding when the magnetic field is applied along the *Z*-axis.[53] This has an important impact on the anisotropy of the magnetic shielding as the MO in Figure 10a will contribute to σ^{p} in the *X* and *Y* directions but not in the *Z* direction. It is therefore likely that this orbital is responsible for a major portion of the chemical shift anisotropy observed experimentally. The four MOs contributing the most to σ^{p}_{iso} also qualitatively illustrate why the CS tensor is close to being axially symmetric. The MOs in Figure 10a and 10b are nearly symmetric about the *Z*-axis while the MOs in Figure 10c and 10d are approximately related by rotational symmetry about the *Z*-axis. Therefore, these four MOs will contribute equally to shielding in both the *X* and *Y* directions; low-lying unoccupied MOs with contributions from all five *d*-orbitals are available to mix with the occupied MOs.

In addition to qualitatively explaining the CS anisotropy and orientation, the MO analysis also suggests that the magnetic shielding is dictated primarily by the V=O bond rather than binding to the dipic and hydroxylamine ligands. In fact, most of the occupied and unoccupied MOs that have significant vanadium *d*-orbital character are primarily centered on the V=O, Figure 10. Except for the MO depicted in Figure 10b, the high energy occupied MOs that represent “bonds” between vanadium and the dipic or hydroxylamine contain very little vanadium *d*-orbital character and are more characteristic of O or N “lone pair” orbitals. This can explain why dipic substitution causes relatively small changes in the vanadium chemical shift tensors. Furthermore, substitution of the hydroxylamido ligands coordinated to the vanadium atom in the V-N-O three membered ring-arrangement is likely to impact the V=O bond more significantly.

Conclusions

Using solid-state NMR spectroscopy we have shown that the electronic environment at the vanadium center in seven coordinate VO(dipic)(ONH_2)(H_2O) complexes is only slightly perturbed when the functionality of the coordinating ligands is changed. While the chemical shift interaction displays measurable yet small variations, the EFG tensor is less responsive. The lack of variation in the EFG tensor suggests that there is minimal change in the local charge distribution close to the vanadium site, possibly suggesting that there is little redistribution of charge in the dipic or hydroxylamine ligands even when the electronic nature of the ligands is significantly altered. These results suggest that ligand functionality in these seven-coordinate vanadium compounds can be tuned without causing a large change in the electrostatic environments. The CS tensor shows minor variations due to ligand substitution which has been attributed to the dominance of the V=O bond in determining the

magnetic shielding of the vanadium. Despite this the CS tensor shows a greater sensitivity than the isotropic chemical shifts obtained from solution ^{51}V NMR.

Acknowledgments

T.P. acknowledges financial support of the National Science Foundation (NSF-CAREER CHE-0237612) and the National Institutes of Health (P20-17716, COBRE individual subproject). K.J.O thanks the Natural Sciences and Engineering Research Council of Canada for financial support. D.C.C acknowledges financial support of the Institute of General Medicine at the National Institutes of Health (GM40525) and the National Science Foundation (CHE-0314719).

References

1. Crans DC, Smee JJ, Gaidamauskas E, Yang L. Chem. Rev. 2004; 104:849–902. [PubMed: 14871144]
2. Thompson KH, Orvig C. Dalton Trans. 2006:761–764. [PubMed: 16437168]
3. Polenova, T.; Pooransingh-Margolis, N.; Renirie, R.; Wever, R.; Rehder, D. Vanadium, The Versatile Metal. Kustin, K.; Crans, DC.; Costa Pessoa, J., editors. Washington: ACS Publications; 2007. In Press
4. Crans DC, Mahroof-Tahir M, Johnson MD, Wilkins PC, Yang L, Robbins K, Johnson A, Alfano JA, Godzala ME III, Austin LT, Willsky GR. Inorg. Chim. Acta. 2003; 356:365–378.
5. Časný M, Rehder D. Chem. Commun. 2001:921–922.
6. Gätjens J, Meier B, Adachi Y, Sakurai H, Rehder D. Eur. J. Inorg. Chem. 2006:3575–3585.
7. Parajón-Costa BS, Piro OE, Pis-Diez R, Castellano EE, González-Baró AC. Polyhedron. 2006; 25:2920–2928.
8. González-Baró AC, Castellano EE, Piro OE, Parajón-Costa BS. Polyhedron. 2005; 24:49–55.
9. Zampella G, Fantucci P, Pecoraro VL, De Gioia L. Inorg. Chem. 2006; 45:7133–7143. [PubMed: 16933914]
10. Zampella G, Fantucci P, Pecoraro VL, De Gioia L. J. Am. Chem. Soc. 2005; 127:953–960. [PubMed: 15656634]
11. Schneider CJ, Zampella G, Greco C, Pecoraro VL, De Gioia L. Eur. J. Inorg. Chem. 2007:515–523.
12. Sakurai H, Tamura A, Takino T, Ozutsumi K, Kawabe K, Kojima Y. Inorg. React. Mech. 2000; 2:69–77.
13. Smee JJ, Epps JA, Teissedre G, Maes M, Harding N, Yang L, Miller SM, Anderson OP, Willsky GR, Crans DC. Manuscript Submitted to Inorg. Chem.
14. Butler A, Clague MJ, Meister G. Chem. Rev. 1994; 94:625–638.
15. Huang W, Todaro L, Francesconi LC, Polenova T. J. Am Chem. Soc. 2003; 125:5928–5938. [PubMed: 12733933]
16. Huang W, Todaro L, Yap GPA, Beer R, Francesconi LC, Polenova T. J. Am Chem. Soc. 2004; 126:11564–11573. [PubMed: 15366903]
17. Skibsted J, Nielsen N Chr, Bildsøe H, Jakobsen HJ. Chem. Phys. Lett. 1992; 188:405–412.
18. Nielsen UG, Jakobsen HJ, Skibsted J. J. Phys. Chem. B. 2001; 105:420–429.
19. Rehder D, Polenova T, Bühl M. Annu. Rep. NMR Spectrosc. 2007:50–116. In Press.
20. Pooransigh-Margolis N, Renirie R, Hasan Z, Wever R, Vega AJ, Polenova T. J. Am. Chem. Soc. 2006; 128:5190–5208. [PubMed: 16608356]
21. Shubin AA, Lapina OB, Bondareva VM. Chem. Phys. Lett. 1999; 302:341–346.
22. Skibsted J, Jacobsen CJH, Jakobsen HJ. Inorg. Chem. 1998; 37:3083–3092.
23. Mackenzie, KJD.; Smith, ME. Multinuclear Solid-State NMR of Inorganic Materials. Oxford: Pergomon; 2002.
24. Crans DC, Felty RA, Chen H, Eckert H, Das N. Inorg. Chem. 1994; 33:2427–2438.
25. Rehder D, Paulsen K, Basler W. J. Magn. Reson. 1983; 53:500–502.

26. Pooransingh N, Pomerantseva E, Ebel M, Jantzen S, Rehder D, Polenova T. Inorg. Chem. 2003; 42:1256–1266. [PubMed: 12588164]
27. Hansen MR, Madsen GKH, Jakobsen HJ, Skibsted J. J. Phys. Chem. B. 2006; 110:5975–5983. [PubMed: 16553406]
28. Rehder, D. Multinuclear NMR. Mason, J., editor. New York: Plenum; 1989. p. 488-493.
29. Ooms KJ, Wasylishen RE. J. Am. Chem. Soc. 2004; 126:10972–10980. [PubMed: 15339183]
30. Feindel KW, Ooms KJ, Wasylishen RE. Phys. Chem. Chem. Phys. 2007; 9:1226–1238. [PubMed: 17325769]
31. Kaupp, M.; Bühl, M.; Malkin, VG., editors. Calculation of NMR and EPR Parameters. Weinheim: Wiley-VCH; 2004.
32. Gee BA. Solid State Nucl. Magn. Reson. 2006; 30:171–181. [PubMed: 17023147]
33. Bühl M, Hamprecht FA. J. Comp. Chem. 1998; 19:113–122.
34. Bühl M, Parrinello M. Chem. Eur. J. 2001; 7:4487–4494. [PubMed: 11695683]
35. Wieghardt K. Inorg. Chem. 1978; 17:57–64.
36. Yang L, La Cour A, Anderson OP, Crans DC. Inorg. Chem. 2002; 41:6322–6331. [PubMed: 12444775]
37. Nuber B, Weiss J. Acta Crystallogr. 1981; B37:947–948.
38. Bradshaw JS, Maas GE, Lamb JD, Izatt RM, Christensen JJ. J. Am Chem. Soc. 1980; 102:467–474.
39. Harris RK, Becker ED, De Menezes SMC, Goodfellow R, Granger P. Pure Appl. Chem. 2001; 73:1795–1818.
40. Bak M, Rasmussen JT, Nielsen NC. J. Magn. Reson. 2000; 147:296–330. [PubMed: 11097821]
41. Frisch, MJ.; Trucks, GW.; Schlegel, HB.; Scuseria, GE.; Robb, MA.; Cheeseman, JR.; Montgomery, JA., Jr; Vreven, T.; Kudin, KN.; Burant, JC.; Millam, JM.; Iyengar, SS.; Tomasi, J.; Barone, V.; Mennucci, B.; Cossi, M.; Scalmani, G.; Rega, N.; Petersson, GA.; Nakatsuji, H.; Hada, M.; Ehara, M.; Toyota, K.; Fukuda, R.; Hasegawa, J.; Ishida, M.; Nakajima, T.; Honda, Y.; Kitao, O.; Nakai, H.; Klene, M.; Li, X.; Knox, JE.; Hratchian, HP.; Cross, JB.; Bakken, V.; Adamo, C.; Jaramillo, J.; Gomperts, R.; Stratmann, RE.; Yazyev, O.; Austin, AJ.; Cammi, R.; Pomelli, C.; Ochterski, JW.; Ayala, PY.; Morokuma, K.; Voth, GA.; Salvador, P.; Dannenberg, JJ.; Zakrzewski, VG.; Dapprich, S.; Daniels, AD.; Strain, MC.; Farkas, O.; Malick, DK.; Rabuck, AD.; Raghavachari, K.; Foresman, JB.; Ortiz, JV.; Cui, Q.; Baboul, AG.; Clifford, S.; Cioslowski, J.; Stefanov, BB.; Liu, G.; Liashenko, A.; Piskorz, P.; Komaromi, I.; Martin, RL.; Fox, DJ.; Keith, T.; Al-Laham, MA.; Peng, CY.; Nanayakkara, A.; Challacombe, M.; Gill, PMW.; Johnson, B.; Chen, W.; Wong, MW.; Gonzalez, C.; Pople, JA. Gaussian 03, Revision C.02. Wallingford, CT: Gaussian, Inc; 2004.
42. Becke AD. J. Chem. Phys. 1993; 98:5648–5652.
43. Lee CT, Yang W, Parr RG. Phys. Rev. B. 1988; 37:785–789.
44. Dennington, R., II; Keith, T.; Millam, J.; Eppinnett, K.; Hovell, WL.; Gilliland, R. GaussView, Version 3.09. Shawnee Mission, KS: Semichem, Inc.; 2003.
45. Glendening ED, Reed AE, Carpenter JE, Weinhold F. NBO Version 3.1.
46. Bohmann JA, Weinhold F, Farrar TC. J. Chem. Phys. 1997; 107:1173–1184.
47. Stark RE, Haberkorn RA, Griffin RG. J. Chem. Phys. 1978; 68:1996–1997.
48. Abragam, A. The Principles of Nuclear Magnetism. Oxford: Oxford University Press; 1961.
49. Duer, M., editor. Solid-State NMR Spectroscopy: principles and applications. Oxford: Blackwell Science; 2002.
50. The α angle obtained directly from SIMPSON ranged from 110 to 140°. The 90° phase shift is a result of SIMPSON defining the EFG components as $|V_{ZZ}|$ $|V_{XX}|$ $|V_{YY}|$.
51. Koller H, Engelhardt G, Kentgens APM, Sauer J. J. Phys. Chem. 1994; 98:1544–1551.
52. Ramsey NF. Phys. Rev. 1950; 78:699–703.
53. Jameson CJ, Gutowsky HS. J. Chem. Phys. 1964; 40:1714–1724.
54. Juranić N. Coord. Chem. Rev. 1989; 96:253–290.
55. Ooms KJ, Wasylishen RE. Can. J. Chem. 2006; 84:300–308.

56. Mason J. Solid State Nucl. Magn. Reson. 1993; 2:285–288. [PubMed: 7804782]

BRIEFS ^{51}V MAS NMR spectroscopy and DFT calculations have been employed to investigate the vanadium environments in a series of hydroxylamido VO-dipicolinate complexes. The computed electric field gradient and chemical shift tensors are in good agreement with the experimental results. The vanadium d_z2 orbital along the V=O bond is a major contributor to the magnetic shielding anisotropy.

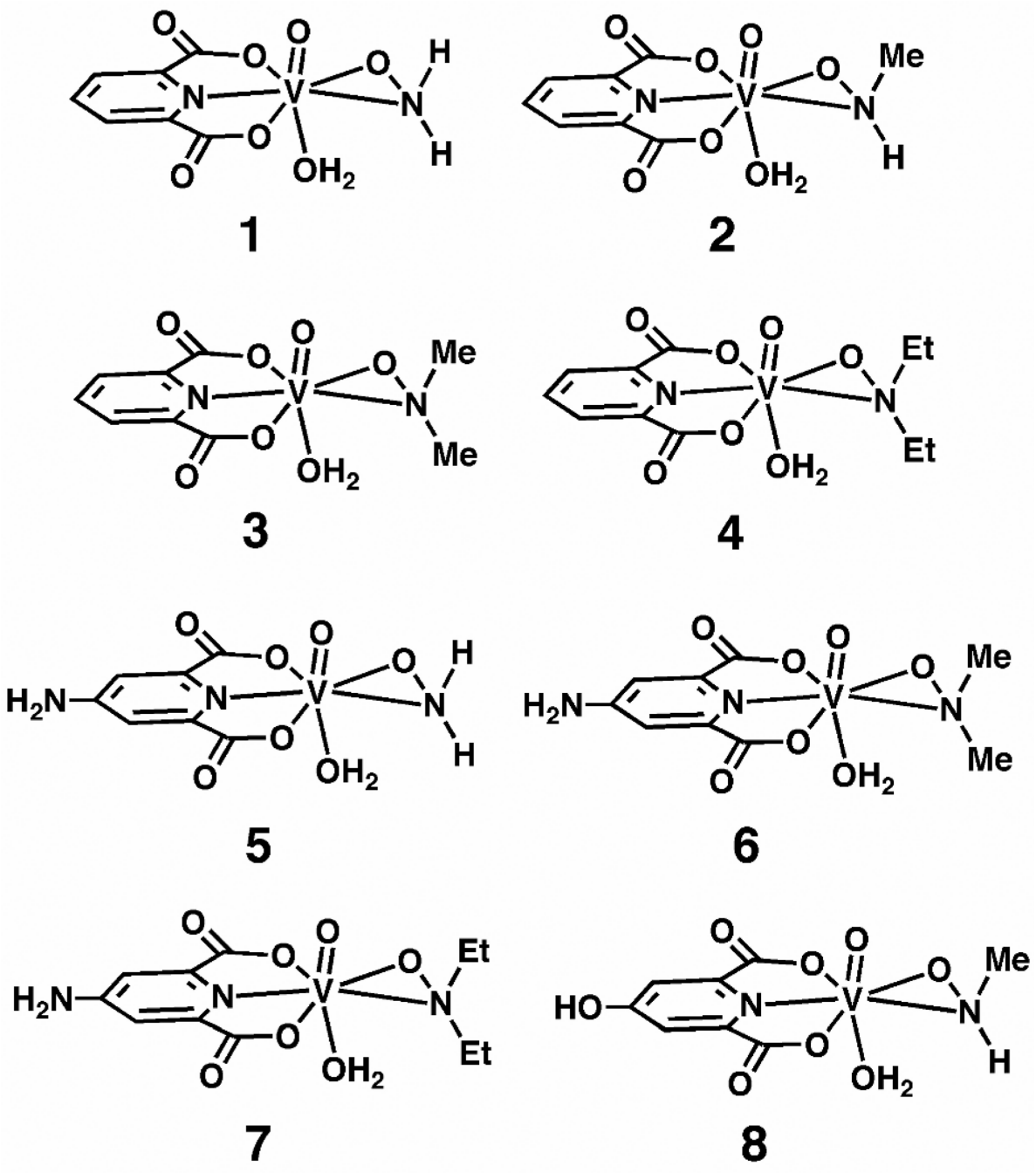

Figure 1.

Schematic representations of the eight vanadium(V) compounds under investigation. [VO(dipic)(ONH_2)(H_2O)] (**1**), [VO(dipic)(ONHMe)(H_2O)] (**2**), [VO(dipic)($ONMe_2$)(H_2O)]·0.5H_2O (**3**), [VO(dipic)($ONEt_2$)(H_2O)] (**4**), [VO(dipic-NH_2)(ONH_2)(H_2O)] (**5**), [VO(dipic-NH_2)($ONMe_2$)(H_2O)]·H_2O (**6**), [VO(dipic-NH_2)($ONEt_2$)(H_2O)] (**7**), [VO(dipic-OH)(ONHMe)(H_2O)]·H_2O (**8**).

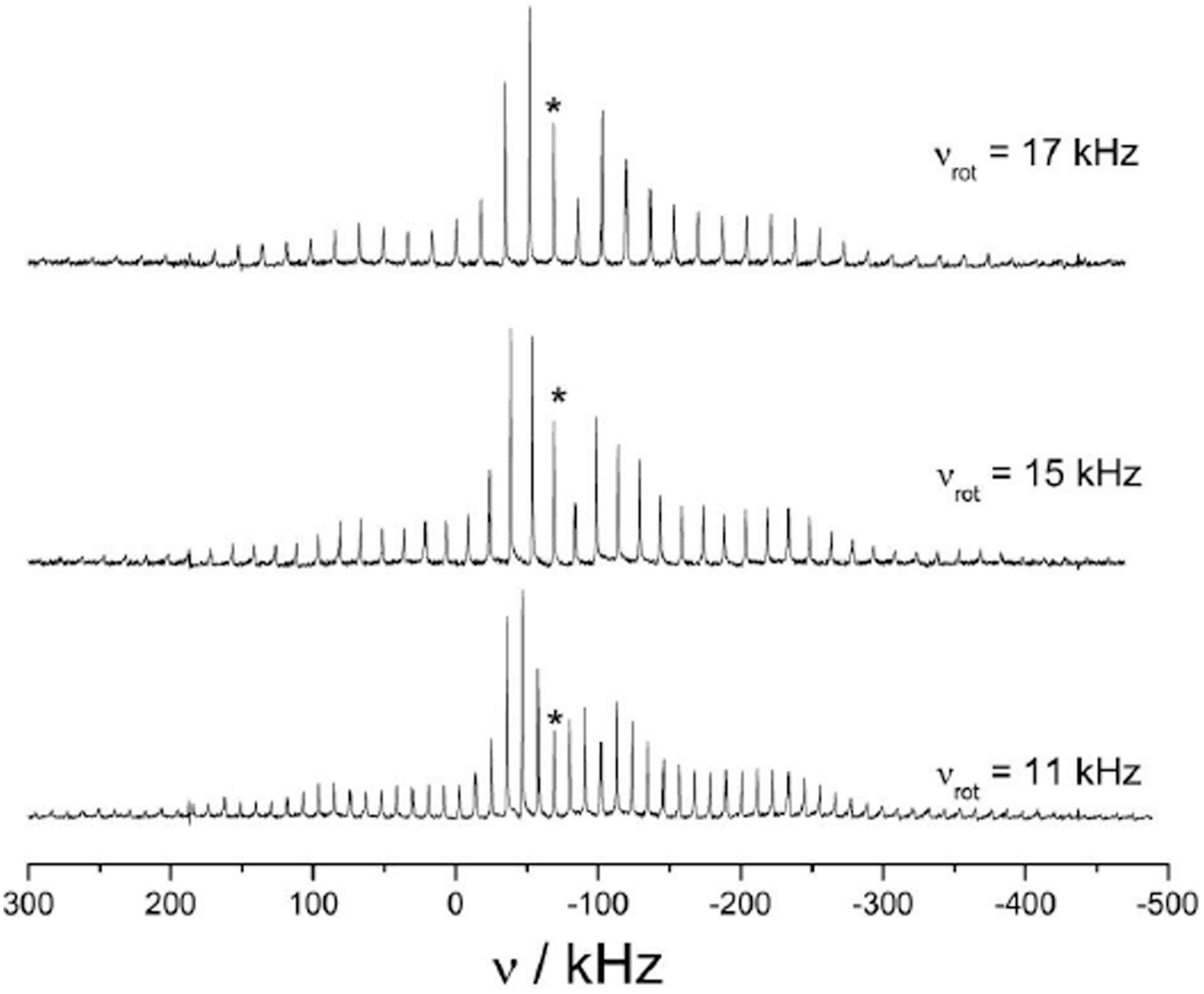

Figure 2.

^{51}V SSNMR spectra of **8** acquired at 9.4 T with MAS rates of 11, 15 and 17 kHz. Each spectrum is the sum of 8192 scans. The asterisk indicates the center-band of the spectrum.

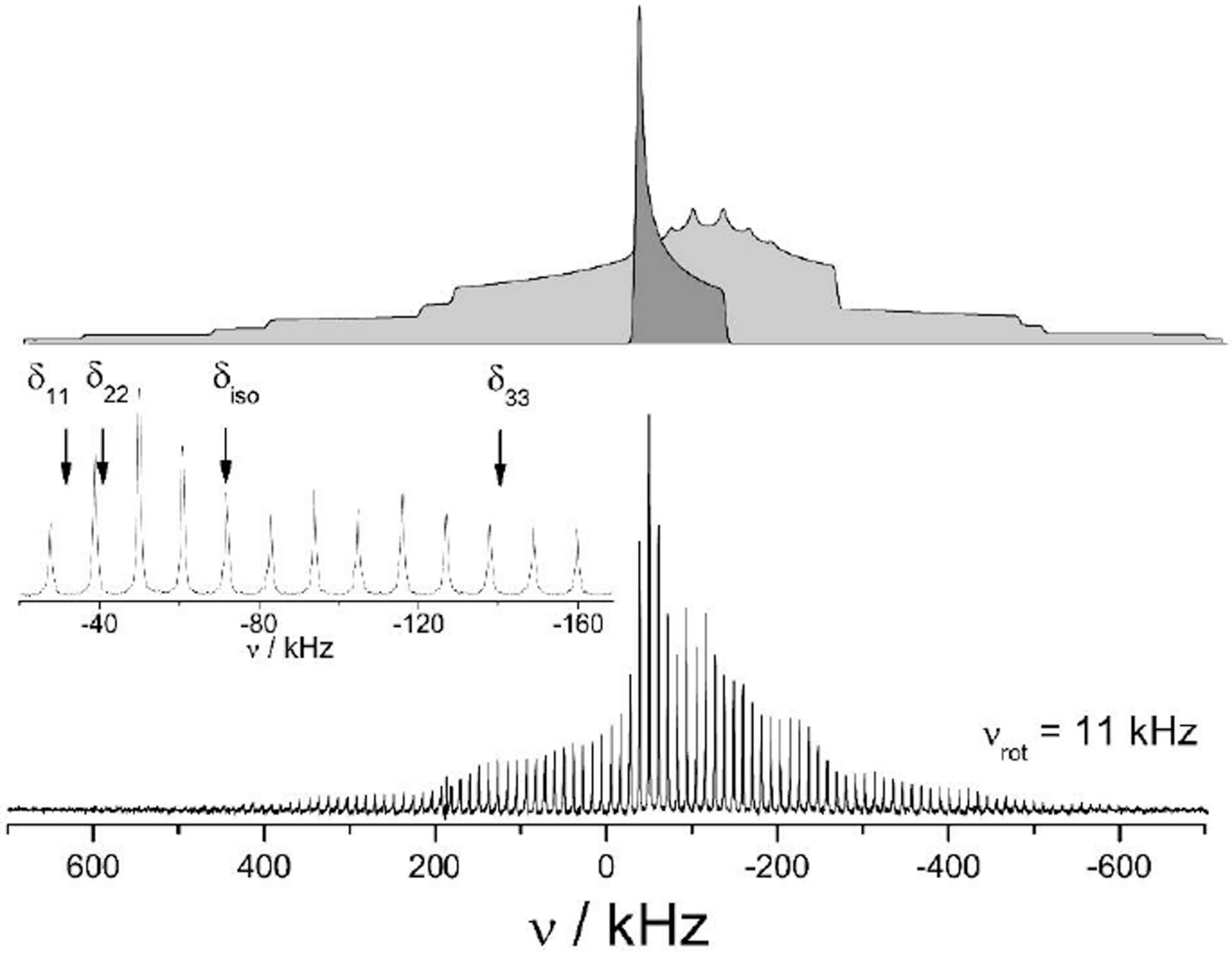

Figure 3.

Bottom: ^{51}V SSNMR spectrum of **1** acquired at 9.4 T with an MAS rate of 11 kHz. The inset spectrum is an expansion of the central transition region of the spectrum illustrating the lack of second-order quadrupolar lineshapes. Top: a stationary spectrum calculated using the parameters in table 1 illustrating the contributions from the central transition (dark grey) and the satellite transitions (light grey). The spinning side band envelope in the experimental spectrum mimics the overall lineshape of these calculated spectra.

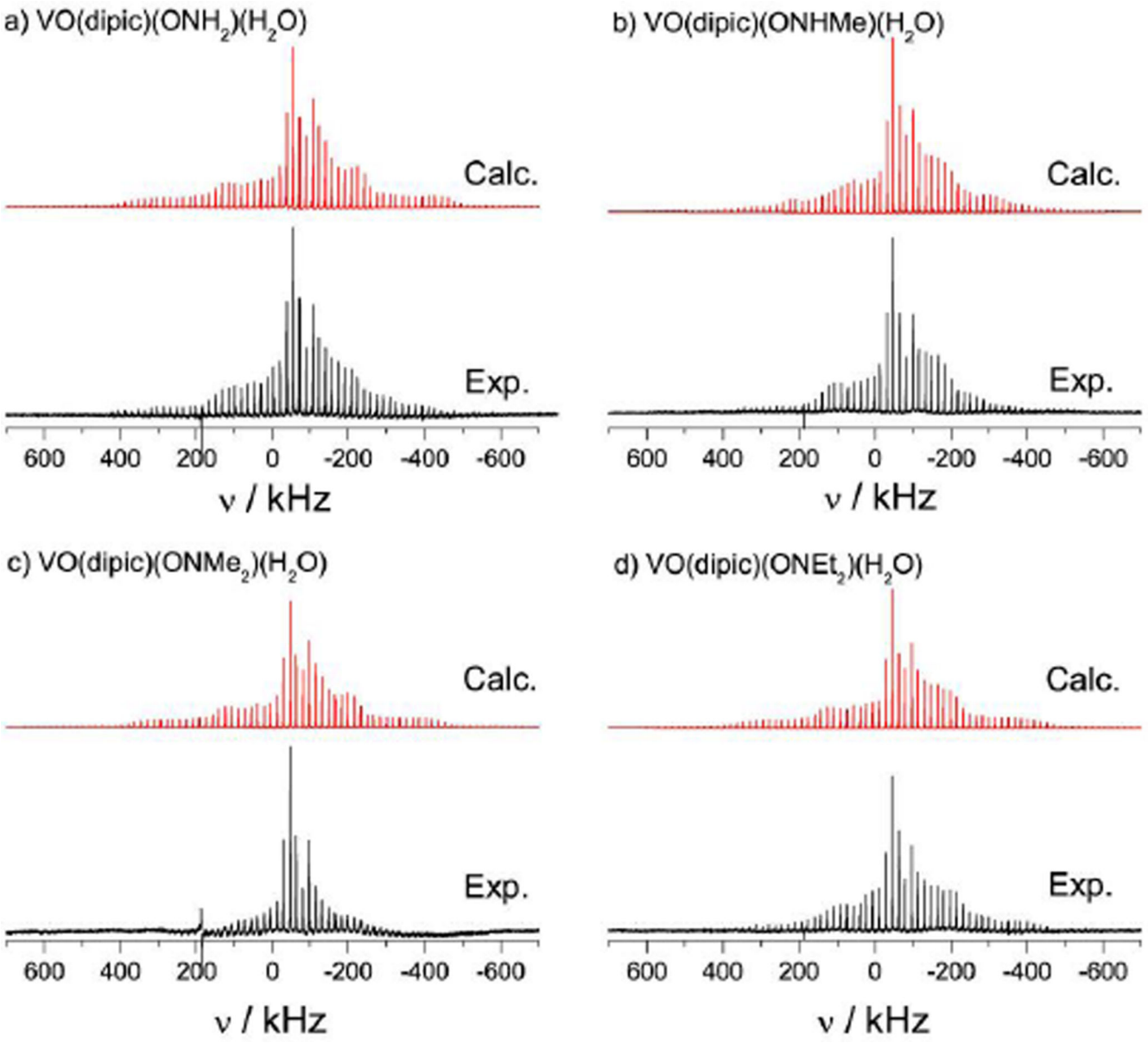

Figure 4.

^{51}V SSNMR spectra of samples of a) **1**, b) **2**, c) **3**, and d) **4**, acquired at 9.4 T with the MAS rate of 17 kHz. The calculated spectra were obtained using the parameters presented in Table 1. Each experimental spectrum is the sum of 8192 scans except for c) which is a sum of 16,384 scans.

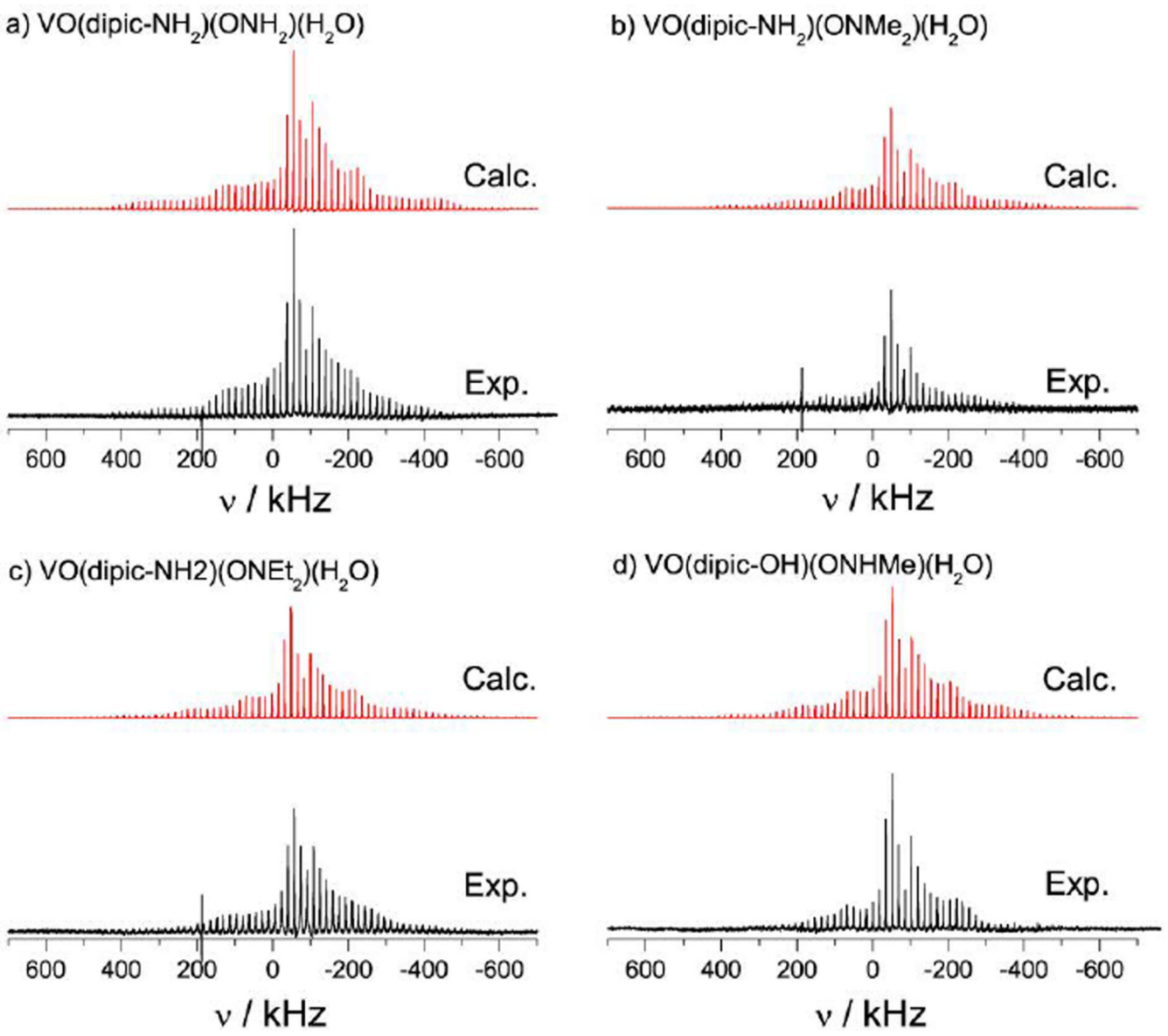

Figure 5.

^{51}V SSNMR spectra of samples of a) **5**, b) **6**, c) **7**, and d) **8**, acquired at 9.4 T with MAS rates of 17 kHz. The calculated spectra were obtained using the parameters presented in Table 1.

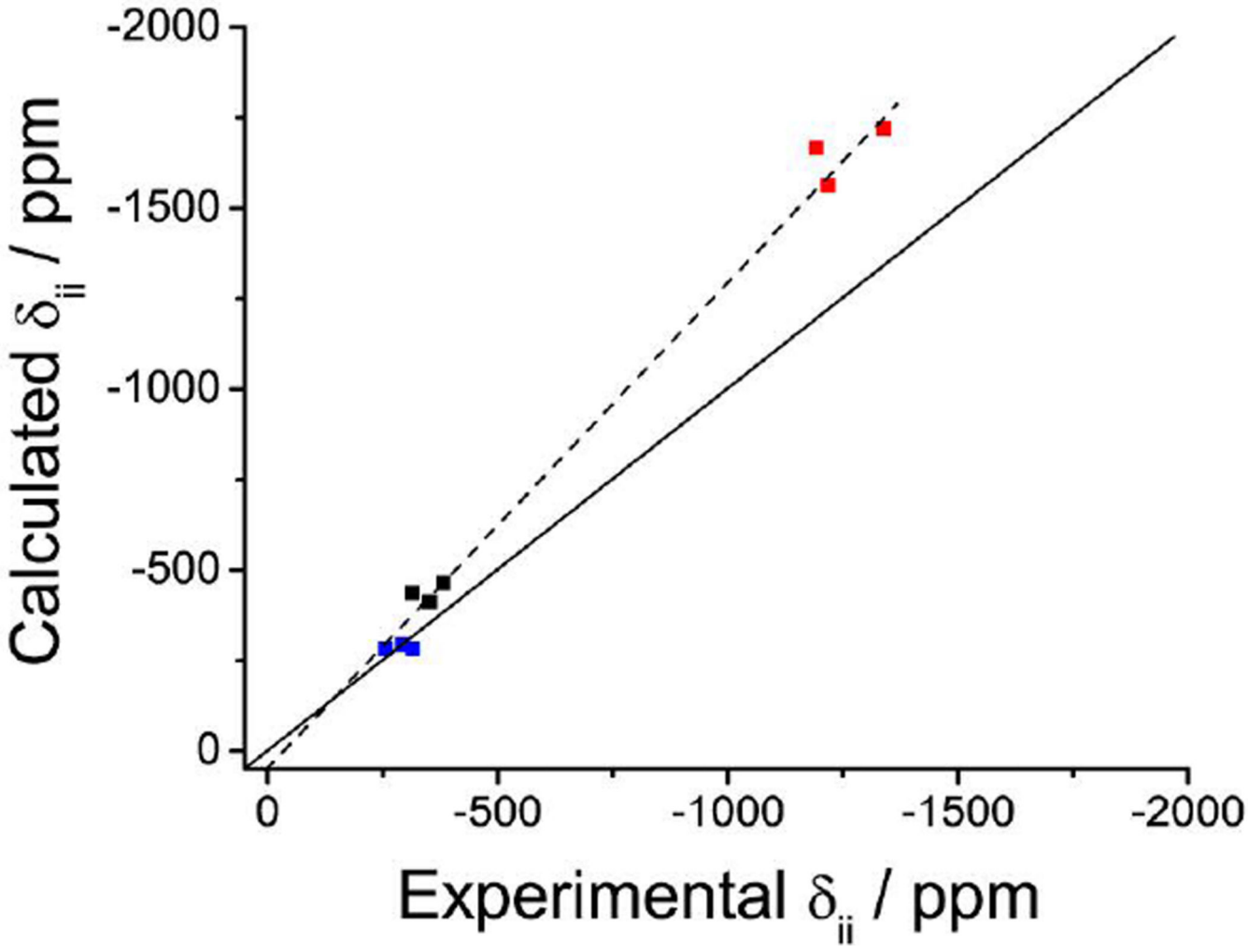

Figure 6.

Plots of the experimental and calculated δ_{ii} values (ii = 11, 22, 33). Solid black line corresponds to perfect agreement, while the dashed black line is the best fit line; δ_{calc}(ppm) = 1.4 δ_{exp}(ppm) + 76, R^2 = 0.99.

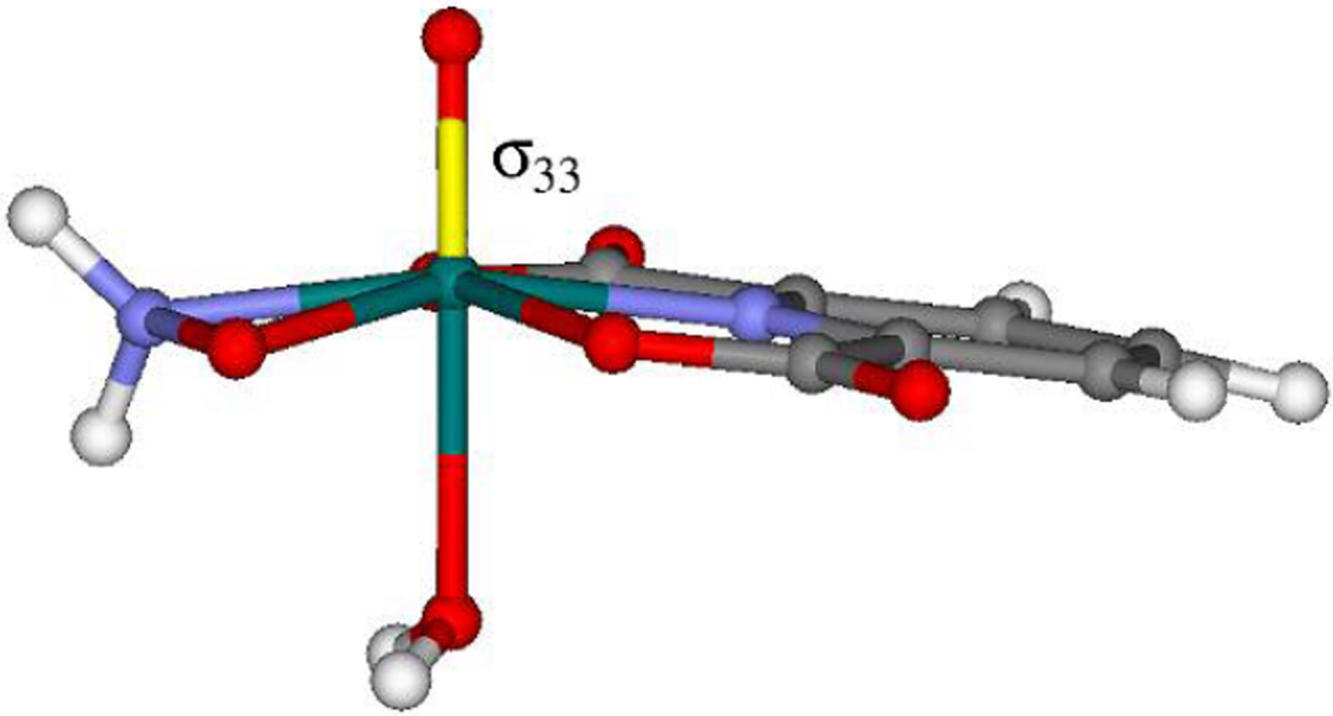

Figure 7.

The molecular structure of **1** obtained from single-crystal x-ray diffraction with the orientation of σ_{33} as predicted by the quantum chemical calculations indicated in yellow.[37] Carbons are grey, hydrogens are white, oxygens are red, nitrogens are blue and vanadium is green.

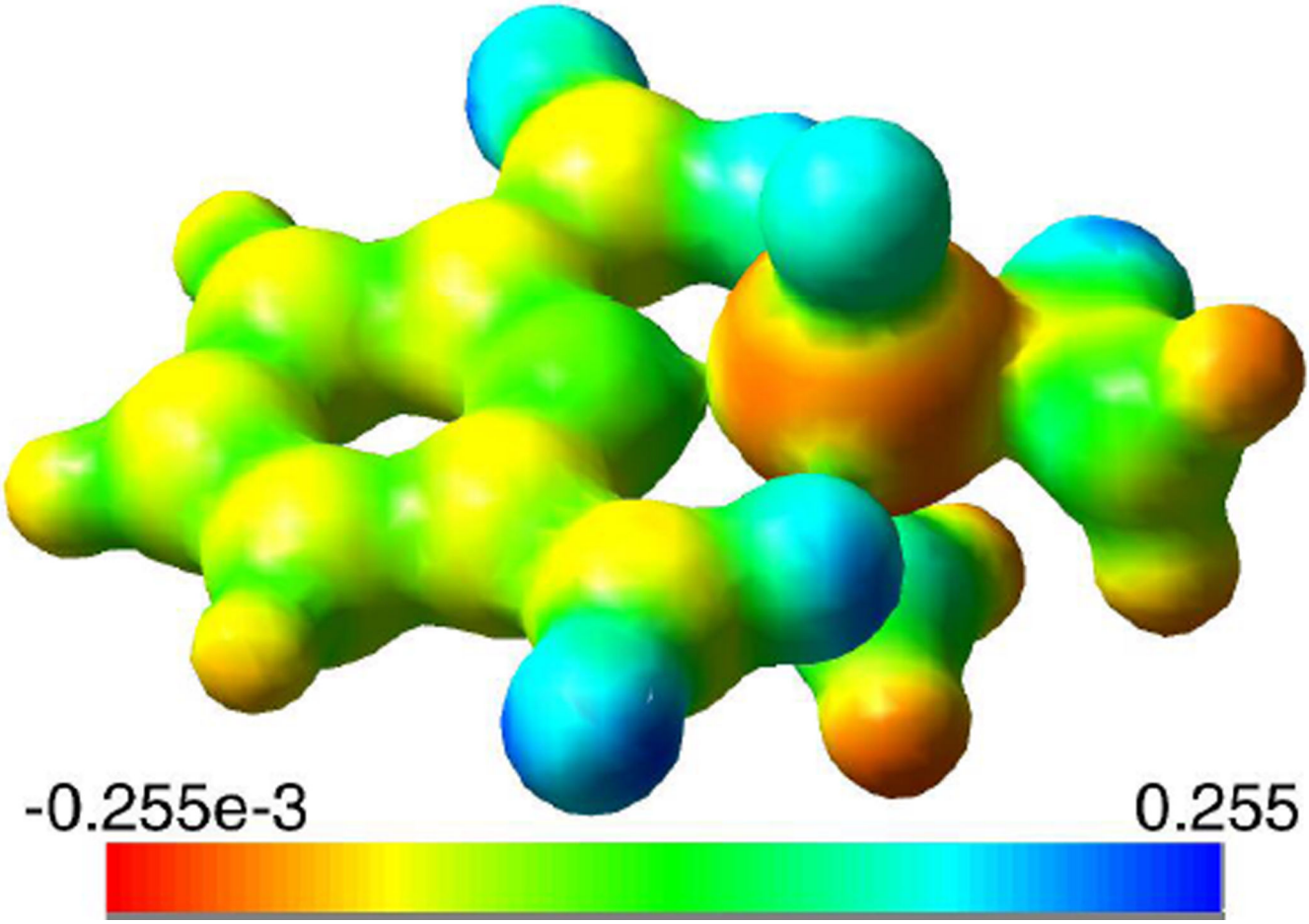

Figure 8.

An image of the electrostatic potential surface of [VO(dipic)(ONH_2)(H_2O)] **(1)** created from the total SCF density calculated in Gaussian. The regions of the positive charges are colored in blue while the regions of the negative charge are depicted in red. The color legend is shown at the bottom.

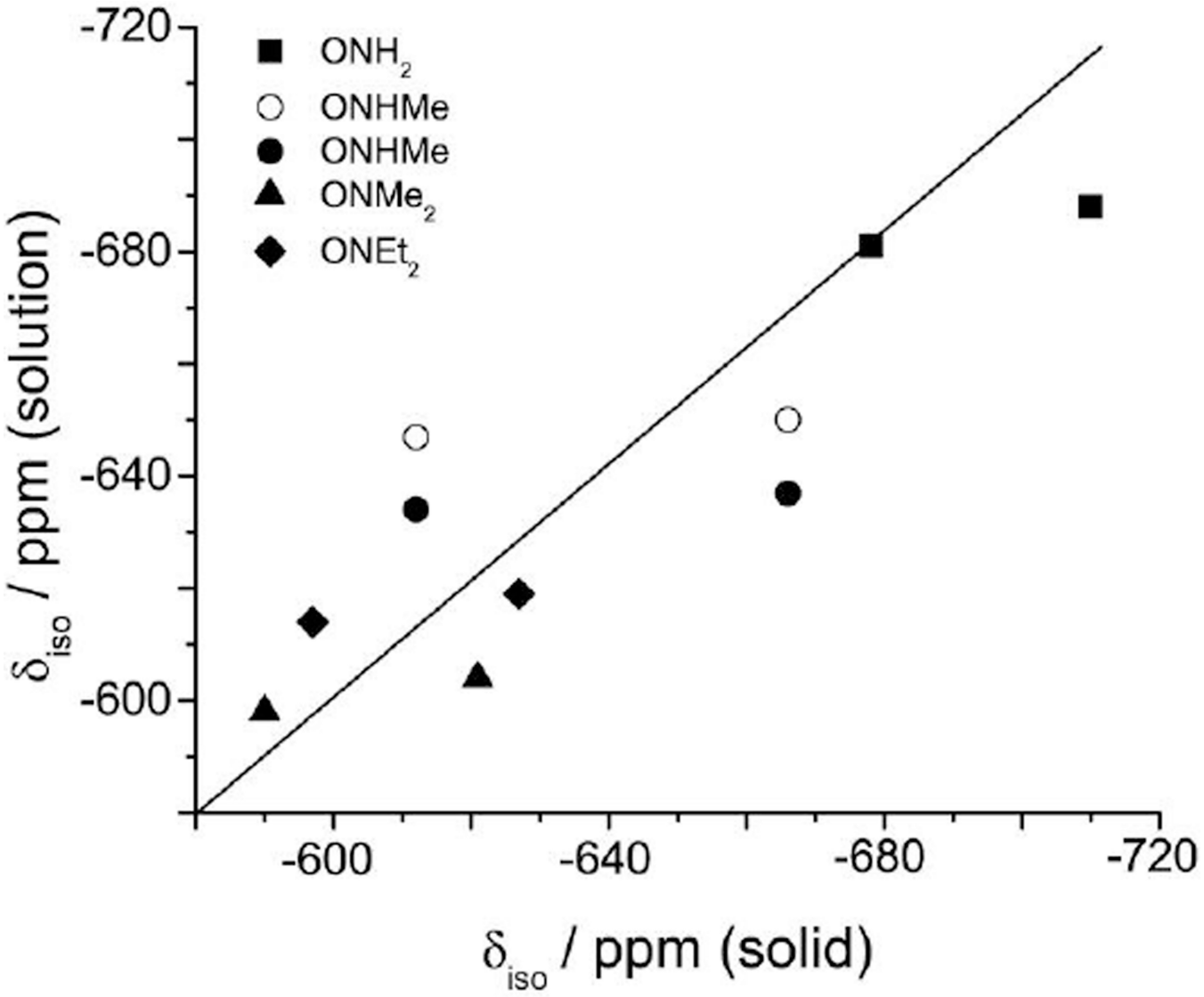

Figure 9.

A plot of the ^{51}V isotropic chemicals shift obtained from solutions NMR vs. that obtained from SSNMR for a series of hydroxylamido vanadium dipicolinate complexes. The compounds are shown presented by the symbol (solid square) are **1** and **4**, (solid circle) are the major component in solution of **2** and **8**, (open circle) are the minor component in solution of **2** and **8**, (solid diamond) are **3** and **5** and (solid triangle) are **4** and **7**. The two symbols solid and open circles of **2** and **8** reflect the fact that there are two isomers of these complexes in aqueous solution. Solid black line corresponds to perfect agreement between solid and solution NMR values.

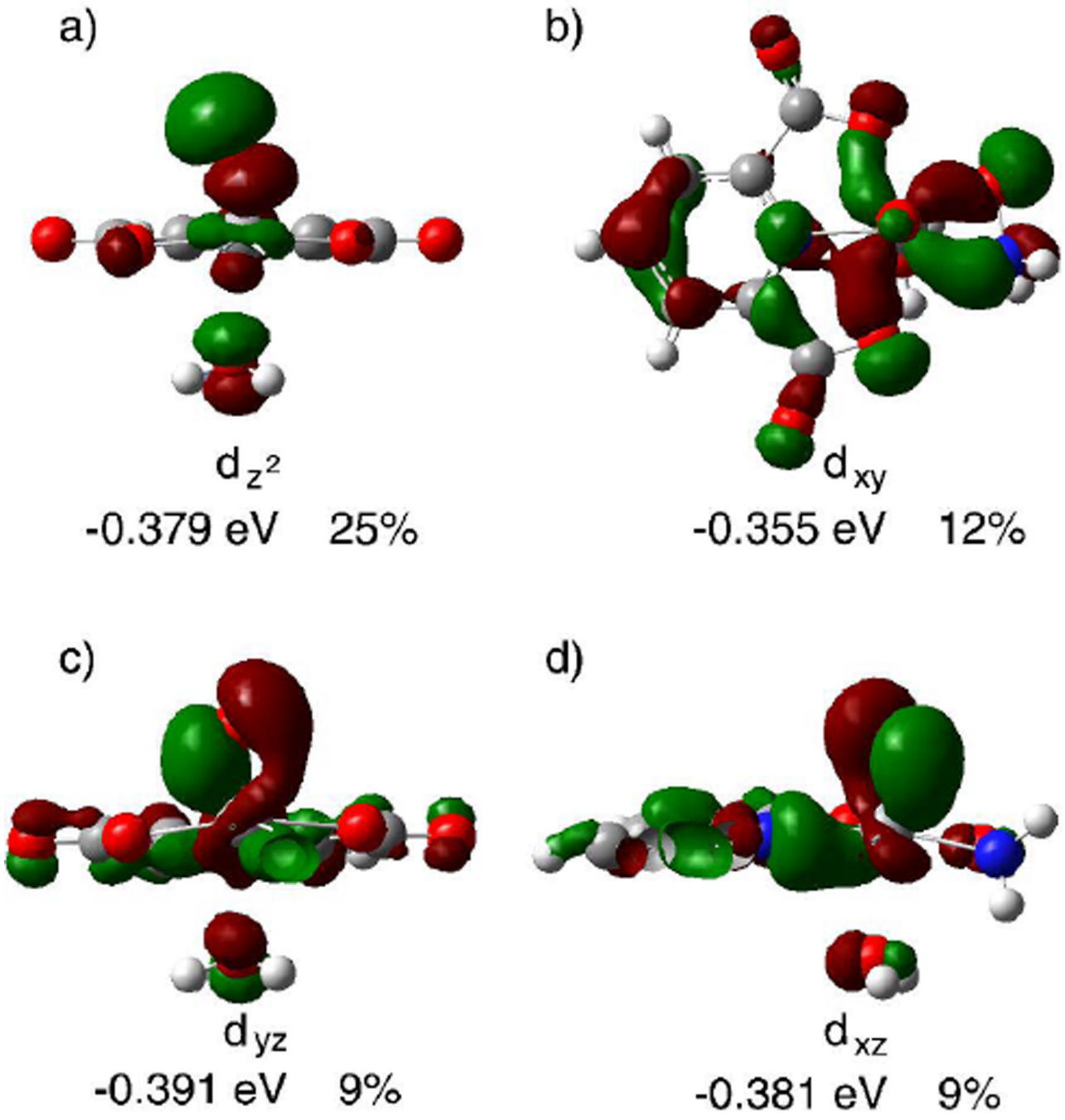

Figure 10.

Four of the MOs obtained from the Gaussian03 calculations that contribute significantly to the calculated paramagnetic shielding and contain significant vanadium *d*-orbital character; contributions are given as a % of the total paramagnetic shielding. The energies of the orbital and % contributions are obtained from the NBO/NCS analysis. The orientation of the molecule is as follows: a) and c) viewed along the V-(dipic-N) bond, b) viewed down the V=O bond, d) viewed perpendicular to both the V=O and V-(dipic-N) bonds.

Table 1

Experimental ^{51}V NMR parameters for solid VO(dipic-*X*)*L*(H_2O) compounds.[1,2]

	X	*L*	C_Q /MHz ± 0.1	η_Q ± 0.0	δ_{iso} / ppm ± 5	δ_{11} / ppm ± 30	δ_{22} / ppm ± 30	δ_{33} / ppm ± 30	α[4]/° ± 30	β[4]/° ± 20	δ_{iso} (solution) / ppm
1	H	ONH_2	3.4	0.8	−678	−315	−381	−1338	20	90	−681
2	H	ONHMe	3.0	0.5	−612	−293	−351	−1192	20	90	−634 / −647
3[3]	H	$ONMe_2$	3.2	0.8	−597	−256	−314	−1217	20	90	−614
4	H	$ONEt_2$	3.3	0.7	−590	−280	−280	−1210	10	90	−598
5	NH_2	ONH_2	3.9	0.8	−710	−314	−386	−1430	40	90	−688
6	NH_2	$ONMe_2$	3.4	0.4	−627	−242	−312	−1327	35	90	−619
7[3]	NH_2	$ONEt_2$	3.5	0.7	−621	−236	−306	−1321	25	90	−604
8	OH	ONHMe	3.2	0.4	−666	−270	−342	−1386	35	90	−637 / −650

[1] The chemical shift parameters are defined such that $\delta_{33} \le \delta_{22} \le \delta_{11}$ and $\delta_{iso} = (\delta_{11} + \delta_{22} + \delta_{33})/3$.[56] The components of the chemical shift tensor are $\delta_{ii} = (\nu_{ii} - \nu_{ref})/\nu_{ref}$ (ii = 11, 22, 33).

[2] The EFG parameters are $C_Q = eQV_{ZZ}/h$ and $\eta_Q = (V_{XX}-V_{YY})/V_{ZZ}$ where $|V_{ZZ}| \ge |V_{YY}| \ge |V_{XX}|$, e is the electron charge and h is Planck's constant.

[3] Due to low signal to noise the errors are approximately 50% greater than reported in the table headings.

[4] The Euler angle γ had no noticeable affect on the NMR lineshapes.

[5] The two chemical shifts listed for samples **2** and **8** arise from the compounds adopting two different conformations in solution.

Table 2

Calculated ^{51}V NMR parameters for solid VO(dipic) *L* (H_2O) compounds.

	L	C_Q / MHz	η_Q	δ_{iso} / ppm	δ_{11} / ppm	δ_{22} / ppm	δ_{33} / ppm
1	ONH_2	3.43	0.68	−822	−282	−464	−1721
2	ONHMe	2.82	0.36	−790	−294	−412	−1666
3	$ONMe_2$	4.09	0.38	−768	−283	−438	−1564